Minimal model of the magnetically induced metal-insulator transition: Finite-temperature properties

M. Dian[1,2] and R. Hlubina[1]

[1]*Department of Experimental Physics, Comenius University, Mlynská Dolina F2, 842 48 Bratislava, Slovakia*

[2]*Department of Theoretical Physics, Comenius University, Mlynská Dolina F2, 842 48 Bratislava, Slovakia*

(Received 31 January 2014; revised manuscript received 3 April 2014; published 21 April 2014)

An unconventional type of metal-insulator transition is realized in the $FeSi_{1-x}Ge_x$ alloys which is driven by the magnetic instability of the paramagnetic insulator. Recently, a minimal model for this type of transition has been introduced and studied in the limit of vanishing temperature. Here we explore the finite-temperature properties of the minimal model in the mean-field approximation. We show that the predictions of the model are in qualitative agreement with experimental data on $FeSi_{1-x}Ge_x$ and on FeGe under pressure.

DOI: 10.1103/PhysRevB.89.155127 PACS number(s): 71.30.+h, 75.30.Kz, 75.50.Bb

I. INTRODUCTION

A large part of modern condensed matter physics concentrates on situations when the presence of electron-electron interactions leads to qualitatively novel phenomena. Interaction-driven transitions from a metal to an insulator, the so-called Mott transitions, are among the most fascinating phenomena of this sort. An outstanding example of the relevance of the Mott transition is provided by the physics of high-temperature cuprate superconductors.

Although many details of the Mott metal-insulator transitions are still under debate, the general picture of such transitions seems to be clear: the metal may become insulating only if the electron-electron interactions become sufficiently strong with respect to the kinetic energy of the electrons. In a sense, this is a quantum analog of the freezing transition: the atoms freeze when the potential energy exceeds the energy of their thermal motion. The insulating state of the electrons at low temperatures usually develops *magnetic order as a consequence of the charge localization*, thereby making the freezing analogy even more precise.

Nevertheless, a completely different type of metal-insulator transition has been experimentally observed in the isoelectronic and isostructural $FeSi_{1-x}Ge_x$ alloys [1,2]. In fact, the end-member FeSi has a smaller lattice constant than the other end-member FeGe; therefore, the kinetic energy of the electrons in FeSi should be larger than in FeGe. On the other hand, since the dominant electronic states in the vicinity of the Fermi level of the alloys are of Fe $3d$ character [3–5], the local electron-electron repulsion should be quite independent of x throughout the whole composition range of $FeSi_{1-x}Ge_x$. Therefore, if there has to be a difference of the electrical properties between FeSi and FeGe, then FeSi should be metallic and FeGe should be insulating. However, the experiment finds the exact opposite: FeSi is insulating and FeGe is metallic!

On the other hand, the evolution of the magnetic properties of $FeSi_{1-x}Ge_x$ with x is quite conventional: the less correlated end-member FeSi is nonmagnetic [6], whereas the more correlated end-member FeGe is magnetically ordered with a large magnetic moment $\sim 1\mu_B$ per Fe atom [7,8]. This observation, therefore, suggests [9] that it is the magnetism which causes the mysterious metal-insulator transition in $FeSi_{1-x}Ge_x$, just the other way round as in the usual case. We are, therefore, confronted with an unconventional type of the metal-insulator transition, which has been dubbed the *magnetically induced metal-insulator transition* [9].

Recently, a fully microscopic minimal model for magnetically induced metal-insulator transitions has been proposed [10]. The ground-state phase diagram of the minimal model has been studied within the mean-field approximation [10] and also making use of correlated variational wave functions [11]. The finite-temperature predictions of the minimal model are presented in this paper. In order to be able to obtain a broad view of the model in a large parameter space, we have chosen to work in the mean-field approximation.

The plan of this paper is as follows. In Sec. II we present the minimal model, specify the parameters for which it will be studied, and introduce the mean-field equations to be solved. In Sec. III we present the finite-temperature phase diagram of the minimal model which consists of the paramagnetic and ferromagnetic phases, and we describe several relevant observables in both phases. Our conclusions are presented in Sec. IV.

II. THE MODEL AND ITS SOLUTION

As described in detail in Ref. [10], the minimal model for the $FeSi_{1-x}Ge_x$ alloys concentrates on the Fe atoms only. The iron atoms are supposed to occupy an fcc lattice, which is a reasonable approximation to the actual locations of the Fe atoms in the B20 structure. The alloys are modeled by a single-band Hubbard model on the fcc lattice with nearest-neighbor hopping amplitude t and on-site repulsion U. Let us label the four sites of the fcc lattice in the simple cubic cell by the index $\lambda = 1,2,3,4$; see Fig. 1. This means that each lattice site $i = (\mathbf{R},\lambda)$ of the fcc lattice is uniquely described by the position of the simple cubic unit cell, $\mathbf{R}$, and by the index λ. In order to allow for the possibility of a band-insulating state, we assume that the on-site lattice potential at one of the four sublattices, say $\lambda = 1$, is different from the remaining sublattices, and we assume that there are two electrons per simple cubic unit cell. If the potential on the $\lambda = 1$ sublattice is sufficiently lower than that on the remaining three sublattices, we can obviously end up with a band insulating state. The Hamiltonian of the minimal model, therefore, reads

$$H = t \sum_{\langle i,j\rangle\sigma} c^\dagger_{i\sigma} c_{j\sigma} + U \sum_i n_{i\uparrow} n_{i\downarrow} + \sum_{i\sigma} (\Delta_i - \sigma B) n_{i\sigma}, \quad (1)$$

where $c^\dagger_{i\sigma}$ creates an electrons at site i, $c_{j\sigma}$ annihilates an electrons at site j, $n_{i\sigma} = c^\dagger_{i\sigma} c_{i\sigma}$, $\sigma = \uparrow,\downarrow$ is the spin index

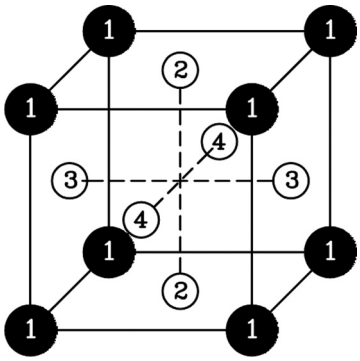

FIG. 1. fcc lattice with two inequivalent types of sites. Black and white sites correspond to $\lambda = 1$ and $\lambda = 2,3,4$, respectively. The on-site lattice potential on the black sites is lower than on the white sites.

and Δ_i is the sublattice potential which equals $-\Delta$ if i lies in the sublattice with $\lambda = 1$; otherwise $\Delta_i = 0$. Note that we have also allowed for external magnetic field B applied along the z axis.

In Ref. [10] it has been argued that the whole series of the $FeSi_{1-x}Ge_x$ alloys can be modeled by Eq. (1) with a positive tunneling matrix element $t \approx 0.25$ eV. It has also been suggested that increasing the Ge content x should be described by increasing the dimensionless interaction strength U/t and that for the potential we should take

$$\Delta/t = 12 - 1.5U/t. \tag{2}$$

Note that for $U/t = 0$, Eqs. (1) and (2) reduce to a tight-binding model for a noninteracting band insulator, whereas for $U/t = 8$ we have to do with the quarter-filled Hubbard model on the usual fcc lattice, which is believed to possess a fully polarized ground state [12,13].

Finite-temperature mean-field solution

In what follows we study the Hamiltonian [Eq. (1)] at a finite temperature T. We make use of the variational formulation of the mean-field theory and we approximate the true interacting Hamiltonian H by a variational Hamiltonian for independent particles H_0. The variational parameters of H_0 will be chosen so as to minimize the following H_0-based estimate of the grand-canonical free energy of the system described by Eq. (1):

$$\Omega(\mu,T,B) = -T\sum_{Q}\ln\left[1+\exp\left(\frac{\mu-\epsilon_Q}{T}\right)\right] + \langle H - H_0\rangle_0,$$

where T is the temperature, μ is the chemical potential, Q labels the single-particle eigenstates of H_0 with eigenenergies ε_Q, and the symbol $\langle\ldots\rangle_0$ denotes a thermal average with respect to H_0.

The variational Hamiltonian H_0 is constructed as follows. Let us first define creation operators for electrons in the Bloch states with wave-vector $\mathbf{k}$ and site index λ on a lattice with L simple cubic unit cells:

$$c^\dagger_{\mathbf{k}\lambda\sigma} = \frac{1}{\sqrt{L}}\sum_{\mathbf{R}} e^{i\mathbf{k}\cdot(\mathbf{R}+\lambda)} c^\dagger_{\mathbf{R}\lambda\sigma}.$$

In terms of these operators, H_0 is defined as

$$H_0 = \sum_{\mathbf{k}\sigma} x^\dagger_{\mathbf{k}\sigma}\mathcal{A}_{\mathbf{k}\sigma}x_{\mathbf{k}\sigma}, \tag{3}$$

where $x^\dagger_{\mathbf{k}\sigma} = (c^\dagger_{\mathbf{k}1\sigma}, c^\dagger_{\mathbf{k}2\sigma}, c^\dagger_{\mathbf{k}3\sigma}, c^\dagger_{\mathbf{k}4\sigma})$ is the four-dimensional row vector of creation operators and $x_{\mathbf{k}\sigma}$ is the conjugate column vector of annihilation operators. The 4×4 matrices $\mathcal{A}_{\mathbf{k}\sigma}$ are given by

$$\mathcal{A}_{\mathbf{k}\sigma} = \begin{pmatrix} e_{1\sigma} & 4tC_xC_y & 4tC_yC_z & 4tC_xC_z \\ 4tC_xC_y & e_{2\sigma} & 4tC_xC_z & 4tC_yC_z \\ 4tC_yC_z & 4tC_xC_z & e_{3\sigma} & 4tC_xC_y \\ 4tC_xC_z & 4tC_yC_z & 4tC_xC_y & e_{4\sigma} \end{pmatrix}, \tag{4}$$

where we have introduced the notation $C_\alpha = \cos(k_\alpha a/2)$, with $\alpha = x,y,z$ labeling the Cartesian components and a standing for the lattice constant of the simple cubic lattice. The diagonal energies $e_{\lambda\sigma}$ are the variational parameters to be optimized.

Let us denote the nth eigenvector of the matrix $\mathcal{A}_{\mathbf{k}\sigma}$ as $\phi_{\mathbf{k}n\sigma}(\lambda)$ and let its eigenvalue be $\varepsilon_{\mathbf{k}n\sigma}$, where $n = 1,\ldots,4$. The single-particle eigenstates of H_0 are, therefore, characterized by $Q = \mathbf{k}n\sigma$, their energy is $\varepsilon_{\mathbf{k}n\sigma}$, and their occupation numbers are given by the Fermi-Dirac distribution $f_{\mathbf{k}n\sigma}$. Minimization of $\Omega(\mu,T,B)$ with respect to $e_{\lambda\sigma}$ yields the conditions

$$e_{\lambda\sigma} = \Delta_\lambda + U\langle n_{\lambda-\sigma}\rangle_0 - \sigma B, \tag{5}$$

where the spin- and orbital-resolved occupation numbers $\langle n_{\lambda\sigma}\rangle_0$ have to satisfy the self-consistent equations

$$\langle n_{\lambda\sigma}\rangle_0 = \frac{1}{L}\sum_{\mathbf{k}n} f_{\mathbf{k}n\sigma}|\phi_{\mathbf{k}n\sigma}(\lambda)|^2. \tag{6}$$

For a given chemical potential μ, we have to solve the coupled set of Eqs. (5) and (6) together with the eigenvalue problem for the real symmetric matrix Eq. (4). Afterwards the chemical potential μ has to be chosen so that

$$\sum_{\lambda\sigma}\langle n_{\lambda\sigma}\rangle_0 = \rho, \tag{7}$$

where for the electron density we take $\rho = 2$.

Throughout this paper, we will assume that the symmetry between the orbitals $\lambda = 2,3,4$ is not spontaneously broken. If we, furthermore, take into account the constraint Eq. (7), then there are only three variational parameters to be optimized. Following Ref. [10], we will make use of the three variational parameters x, m_1, and m_2, in terms of which we can write

$$\langle n_{1\sigma}\rangle_0 = \frac{\rho}{8} + 3x + \sigma m_1, \quad \langle n_{2\sigma}\rangle_0 = \frac{\rho}{8} - x + \sigma m_2.$$

The Helmholtz free energy in the mean-field approximation reads as $F(N,T,B) = \Omega(\mu,T,B) + \mu N$, where $N = \rho L$ is the total electron number. When expressed per simple cubic unit cell, this can be written as

$$f(\rho,T,B) = -\frac{T}{L}\sum_{\mathbf{k}n\sigma}\ln\left[1+\exp\left(\frac{\mu-\epsilon_{\mathbf{k}n\sigma}}{T}\right)\right] + \rho\mu - U\sum_{\lambda}\langle n_{\lambda\uparrow}\rangle_0\langle n_{\lambda\downarrow}\rangle_0. \tag{8}$$

On the other hand, the internal energy per unit cell $u = \frac{1}{L}\langle H\rangle_0$ is easily found to be given by the expression

$$u(\rho,T,B) = \frac{1}{L}\sum_{\mathbf{k}n\sigma}\epsilon_{\mathbf{k}n\sigma}f_{\mathbf{k}n\sigma} - U\sum_{\lambda}\langle n_{\lambda\uparrow}\rangle_0\langle n_{\lambda\downarrow}\rangle_0.$$

Making use of the expressions for $f(\rho,T,B)$ and $u(\rho,T,B)$ we can calculate the specific heat per unit cell in two alternative ways:

$$c = -T\frac{\partial^2 f}{\partial T^2} = \frac{\partial u}{\partial T}.$$

Other physical observables which we will be interested in include the total magnetization per unit cell

$$m = m_1 + 3m_2,$$

the uniform magnetic susceptibility

$$\chi = 2\frac{\partial m}{\partial B} = -\frac{\partial^2 f}{\partial B^2}, \tag{9}$$

and the inverse electronic compressibility

$$\frac{1}{\kappa} = \frac{\partial \mu}{\partial \rho} = \frac{\partial^2 f}{\partial \rho^2}. \tag{10}$$

The mean-field problem posed by Eqs. (4), (5), and (6) has been solved numerically on finite lattices with periodic boundary conditions. Typically we have studied $L = 127 \times 127 \times 127$ unit cells. In order to speed up the calculations, we have made use of the point-group symmetries of the minimal model.

III. RESULTS

A global scan of the finite-temperature phase diagram along the line defined by Eq. (2) shows only two thermodynamic phases which are distinguished by whether the magnetization m is finite or not; see Fig. 2. Note that, as expected, the magnetic phase diagram is quite conventional: magnetic ordering starts at the critical interaction $U_c/t \approx 3.494$ and its critical temperature grows with increasing U. In Ref. [10] it has been suggested that the quantum critical point at $U = U_c$ corresponds to the experimentally determined transition in the $FeSi_{1-x}Ge_x$ alloys, observed at $x_c \approx 0.25$ [1], from the paramagnetic insulator at $x < x_c$ to the ferromagnetic metal at $x > x_c$. In the rest of this section we shall study the physical properties of the paramagnetic and ferromagnetic phases, concentrating not only on their magnetic, but also on their electric and thermal properties.

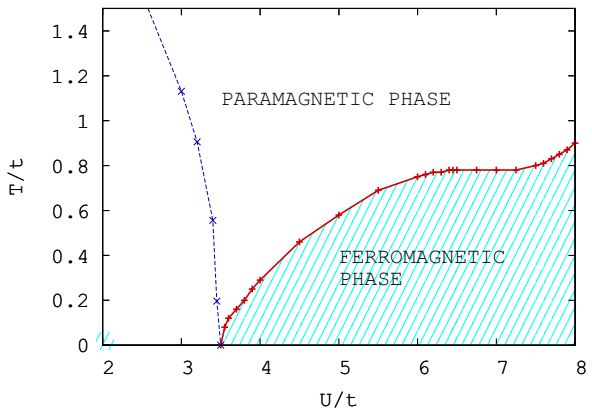

FIG. 2. (Color online) Finite-temperature phase diagram of the minimal model along the line defined by Eq. (2). The dotted line shows the locations of the maxima in the temperature dependence of the uniform susceptibility χ in the paramagnetic state.

A. Paramagnetic phase

Let us start by discussing the results for the magnetic susceptibility χ in the paramagnetic phase; see Fig. 3. Note that in the low-temperature limit, χ vanishes for all $U < U_c$, as expected for an insulating ground state [10]. Less obvious is the finite-temperature behavior of χ: as U approaches U_c, the susceptibility develops a large peak at intermediate temperatures. The peak height grows and its position shifts to lower temperatures for increasing U. For U close to U_c the susceptibility predicted by the minimal model becomes qualitatively similar to the experimental data on FeSi [6]; see Fig. 4. Within the minimal model, the peak of the susceptibility is obviously caused by the vicinity to the ordered phase (see Fig. 2), since at the paramagnetic-ferromagnetic boundary the susceptibility has to diverge. Our explanation of the anomalous behavior of FeSi is, therefore, conceptually similar to the nearly magnetic point of view of Refs. [14–16].

The electronic compressibility κ which is also plotted in Fig. 3 shows similar behavior to that of the magnetic susceptibility χ, but with less pronounced peaks at intermediate temperatures. The difference between κ and χ becomes qualitative only on the metallic side $U > U_c$: the magnetic susceptibility diverges for $T \to 0$, whereas the electronic

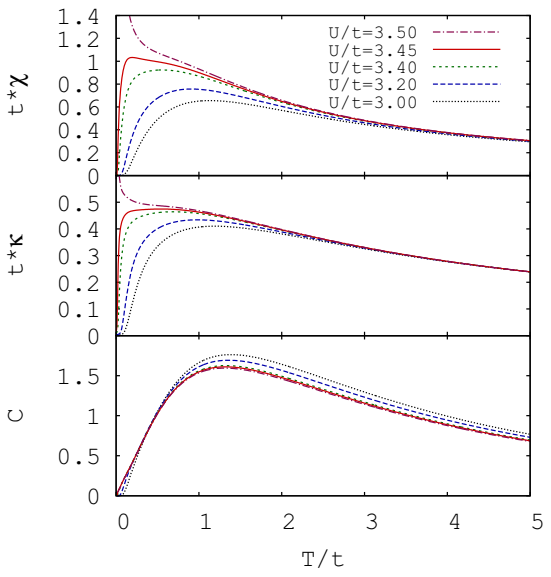

FIG. 3. (Color online) Magnetic susceptibility χ (top panel), electronic compressibility κ (middle panel), and specific heat c (bottom panel) as functions of temperature for several values of U. Note that for $U/t = 3.5$ the system is already ferromagnetic and its susceptibility χ diverges as $T \to 0$.

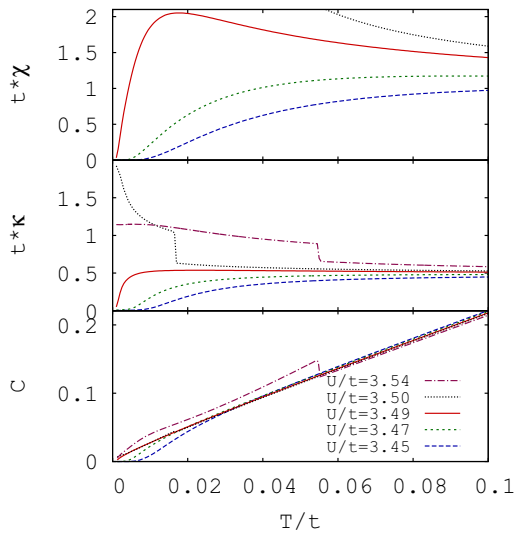

FIG. 4. (Color online) A detailed view of the same observables as in Fig. 3 for $U \sim U_c$ in the limit of low temperatures.

compressibility stays finite in this limit, as should have been expected.

It is worth pointing out that, for $U > U_c$, κ exhibits jumps at the critical temperature T_c. If T_c is a function of ρ, this is readily understood within the Landau theory with an order parameter m,

$$f = \alpha(T - T_c)m^2 + \frac{\beta}{2}m^4 - 2mB, \tag{11}$$

since in that case the inverse electronic compressibility Eq. (10) does possess a jump with magnitude

$$\frac{\Delta(\kappa^{-1})}{\Delta c} = -\frac{1}{T_c}\left(\frac{\partial T_c}{\partial \rho}\right)^2,$$

where Δc is the specific-heat jump. The numerical data presented in Fig. 4 is perfectly consistent with this scaling relation.

In order to avoid misunderstandings, let us note that the electronic compressibility κ is quite different from the compressibility of the crystal β. The electronic compressibility κ characterizes the metallicity of the sample, since it measures the changes of the electron density with changing chemical potential in a rigid crystal, and is in principle observable by measuring the screening length. On the other hand, the compressibility β measures how the volume of the crystal changes with the applied pressure and it is not studied in this paper.

In Figs. 3 and 4 we show that the specific heat c changes only little with U for $U \sim U_c$. All $c(T)$ curves exhibit a peak at $T \sim t$ which divides the universal high-temperature region where ultimately $c \propto T^{-2}$ from the low-temperature region where qualitative changes with U occur only at the lowest temperatures. Thus there is a big difference between the evolution with U of c on one hand and of χ and κ on the other hand. This is a hallmark of interaction effects.

It is worth pointing out that, for $U \lesssim U_c$, we do not find an additional peak of the specific heat at temperatures $T < t$. This disagrees with the analysis of the specific heat data for FeSi in Ref. [6], where it was assumed that the phonon contributions to the specific heat $c_{\rm ph}$ are identical in FeSi and CoSi and as a consequence a peak of the electronic contribution $c_{\rm el}$ was found close to 300 K. This procedure has been taken for granted also in most of the later papers on FeSi. However, a refined analysis of $c_{\rm el}$ has been presented more recently [17], where only the same *shape* of the function $c_{\rm ph}(T)$ for FeSi and CoSi has been assumed, and a change of the overall *energy scale* (Debye energy) has been allowed for. Also the contribution of the conduction electrons to the specific heat of CoSi has been taken into account. Such improved analysis led to a function $c_{\rm el}(T)$ for FeSi whose dominant feature was the presence of a gap below $\approx$200 K and a mild temperature dependence at higher temperatures, much closer to what we find than the older analysis of Ref. [6].

In view of the very recent discovery of a quite different temperature dependence of the elastic constants in FeSi and CoSi [18], it seems to be very likely that not even the shape of the functions $c_{\rm ph}(T)$ needs to be the same in FeSi and CoSi and, therefore, even the improved analysis of Ref. [17] does not need to be correct. Therefore, in our opinion, the experimental problem of finding $c_{\rm el}(T)$ in FeSi is still open. The most reliable procedure for subtracting the phonons would make use of a direct determination, by means of inelastic neutron scattering, of the phonon density of states in FeSi.

We have found that the single-particle spectrum exhibits quite strong dependence on temperature for all values of $U \lesssim U_c$. Such temperature dependence of the band structure should be observable also in spectroscopic measurements; therefore we have calculated the real part of the optical conductivity $\sigma(\omega)$. For the sake of simplicity, we have neglected the $\mathbf{k}$ dependence of the dipole matrix elements and we have used the formula

$$\sigma(\omega) \propto \frac{1}{\omega L}\sum_{m,n}\sum_{\mathbf{k}\sigma}(f_{\mathbf{k}n\sigma} - f_{\mathbf{k}m\sigma})\delta(\varepsilon_{\mathbf{k}m\sigma} - \varepsilon_{\mathbf{k}n\sigma} - \hbar\omega).$$

The result of this calculation is shown in Fig. 5. We emphasize that our $\sigma(\omega)$ should not be directly compared to experiments, because the high-energy spectrum of the minimal model obviously can not be realistic. What we would like to illustrate

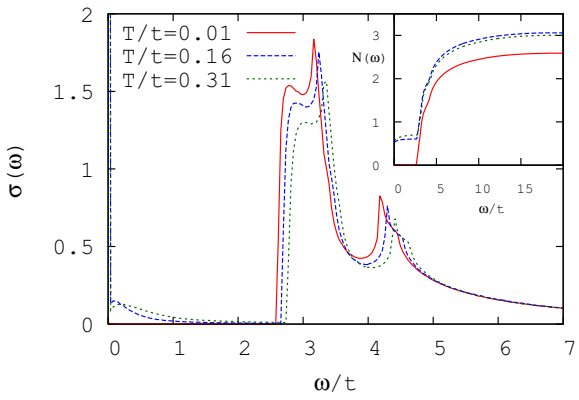

FIG. 5. (Color online) Optical conductivity $\sigma(\omega)$ of the minimal model for $U/t = 3.4$ at several temperatures. The inset shows the restricted sum-rule function $\mathcal{N}(\omega)$ for the same parameters. Both $\sigma(\omega)$ and $\mathcal{N}(\omega)$ are plotted in arbitrary units.

by Fig. 5 are three qualitative aspects of $\sigma(\omega)$, which we believe to be robust:

(i) The direct optical gap is larger than the indirect gap which determines the low-temperature thermodynamic properties. Its magnitude may be reduced by including longer-range hoppings in Eq. (1), but in order to keep the number of parameters small, we do not take such hoppings into account.

(ii) The optical spectra change with temperature even at frequencies $\hbar\omega \approx 4t$ much larger than the temperature scale. Such behavior has in fact been observed in optical studies of FeSi [19] and it has been cited as evidence for strong correlations [20].

(iii) The results for the restricted sum-rule function $\mathcal{N}(\omega) = \int_0^\omega d\nu\sigma(\nu)$ shown in Fig. 5 remind us of the fact, well known in the context of the high-temperature cuprate superconductors, that the optical sum rule in an interacting system may be temperature dependent even for a large cut-off energy Λ. Therefore, the values of $\mathcal{N}(\omega)$ at different temperatures do not have to converge to each other with increasing ω, as has been assumed in the experimental papers [19,20].

To summarize, the absence of the Drude peak in $\sigma(\omega)$ and the vanishing of the electronic compressibility κ, both at $T = 0$, clearly show that the paramagnet has an insulating ground state. As soon as the temperature becomes finite, the paramagnet acquires a finite compressibility κ and is technically metallic. Only first-order transitions could be present within the paramagnet, but at the mean-field level we have found none.

B. Ferromagnetic phase

Before discussing the properties of the ferromagnetic phase in more detail, a word of caution is in place. Namely, in reality FeGe is not a simple ferromagnet as predicted by the minimal model. In fact, due to the lack of inversion symmetry of the B20 structure, the Dzyaloshinskii-Moriya interaction leads to an instability of the putative ferromagnet towards the formation of long-range spirals [21] which exhibit a surprisingly rich phenomenology in applied magnetic fields [22]. However, since the observed period of spiraling in FeGe is large, $\sim$700 Å [23], to a first approximation we shall approximate the helical state by a simple ferromagnet. In principle it is possible to include the weak Dzyaloshinskii-Moriya interaction later as a perturbation to the minimal model.

Returning to the minimal model, in Fig. 6 we plot the magnetization m as a function of temperature for several values of U/t in the ferromagnetic phase. Previous work at $T = 0$ has found a second critical interaction, $U_N/t \approx 6.4$, which divides the region with partially polarized ground states at $U < U_N$ from the fully polarized Nagaoka state at $U > U_N$ [10]. Figure 6 confirms this result and it shows that, in the vicinity of $U = U_N$, a qualitative change of the magnetization curves $m = m(T)$ takes place. It is worth remarking that a somewhat similar change of the magnetization curves has in fact been observed at $x_N \approx 0.4$ in the $FeSi_{1-x}Ge_x$ alloys [1].

Let us further remark that the chemical pressure experienced on FeGe by replacing some of the Ge atoms with the smaller Si atoms can be alternatively realized, without introducing additional disorder, by high-pressure experiments. In such experiments on FeGe, a quantum phase transition

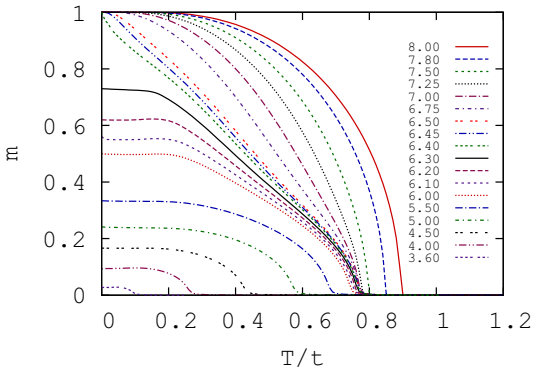

FIG. 6. (Color online) Magnetization m as a function of temperature for several values of U/t.

between two metallic states has been found in the vicinity of 19 GPa [24]. Within our minimal model, this transition can be naturally interpreted as a consequence of a cusp in the pressure dependence of the zero-temperature magnetization $m(0)$ [10,11]; see Fig. 7. It is worth pointing out that also according to recent *ab initio* calculations, the ordered moment of FeGe decreases for pressures close to p_c [5,25]. A similar picture has been suggested in *ab initio* studies of metamagnetism in FeSi as well, which find, in between the paramagnetic insulator and the large-moment metal, a small-moment metallic phase at intermediate magnetic fields [26]. Very recently the interpretation in terms of a Lifshitz transition between partially and fully polarized states has been supported by a detailed study of the pressure dependence of the residual resistivity [27], which is the quantity which has actually been measured in Ref. [24].

As already mentioned, the insulator-to-metal transition in the $FeSi_{1-x}Ge_x$ alloys represents an unconventional universality class, in which the charge delocalization is driven by a magnetic instability of the insulator. In order to facilitate a comparison with the more standard metal-insulator transitions, let us study the predictions of the minimal model for the evolution of the physical properties of the metal, starting at large interactions U and decreasing their value towards U_c.

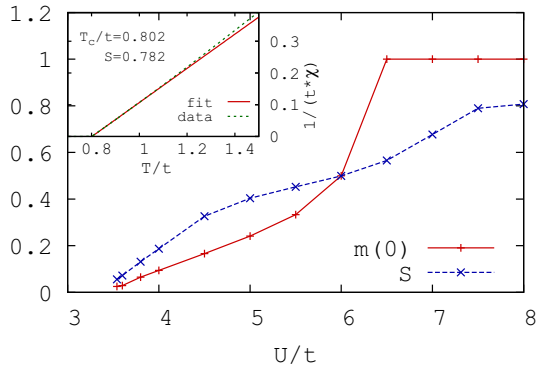

FIG. 7. (Color online) Fluctuating moment S and the low-temperature ordered moment $m(0)$ as functions of U/t. The inset shows the fit of $\chi^{-1}(T)$ for $U/t = 7.5$ making use of Eq. (12).

The question is: how does the metal become insulating as $U \to U_c$?

To answer this question, let us start by comparing the ordered moment $m(0)$ per simple cubic unit cell, in the limit of vanishing temperature, with the fluctuating moment S of the unit cell at temperatures T slightly above T_c. In experimental papers S is determined from the fit

$$\frac{1}{\chi} = \frac{3}{4S(S+1)}(T - T_c). \tag{12}$$

This form follows from Eqs. (9) and (11) which imply $\chi^{-1} = \frac{\alpha}{2}(T - T_c)$, if the constant $\frac{\alpha}{2}$ is interpreted in terms of the local-moment paramagnetism. In Fig. 7 we plot the variation of S and $m(0)$ as functions of U. Note that there is no simple relation between S and $m(0)$, as should have been expected in an itinerant system. In the fully saturated region $U > U_N$ we find that S is smaller than $m(0)$ and comparable to its high-temperature value $S_\infty \approx 0.67$, which does not depend on U and is given only by the band filling. On the other hand, as U approaches U_c, the fluctuating moment S decreases, but the ordered moment $m(0)$ is even smaller. These findings suggest that the metal-insulator transition is driven by the disappearance of charge carriers in the limit $U \to U_c$.

In order to support this point of view, in Fig. 8 we plot, as functions of U, several low-temperature characteristics of the metallic state: the density of states at the Fermi level $N(0)$, the electronic compressibility $\kappa(0)$, and the Fermi volume Ω defined as $\Omega = \sum_{n\sigma} \min(\Omega_{n\sigma}, 1 - \Omega_{n\sigma})$ where $\Omega_{n\sigma} = \frac{1}{L}\sum_{\mathbf{k}} f_{\mathbf{k}n\sigma}$ is the occupation of the band $n\sigma$. It should be pointed out that $N(0)$ is directly measurable via the linear-in-T coefficient of the specific heat $\gamma = \lim_{T\to 0} \frac{c(T)}{T}$. In Ref. [1] it has been found that the coefficient γ of the $FeSi_{1-x}Ge_x$ alloys exhibits a large enhancement for intermediate concentrations $x_c \lesssim x \lesssim x_N$, in good qualitative agreement with the data shown in Fig. 8 [28]. This result can be easily interpreted in terms of the Fermi volume Ω (see Fig. 8), which also exhibits a maximum at intermediate values of U/t.

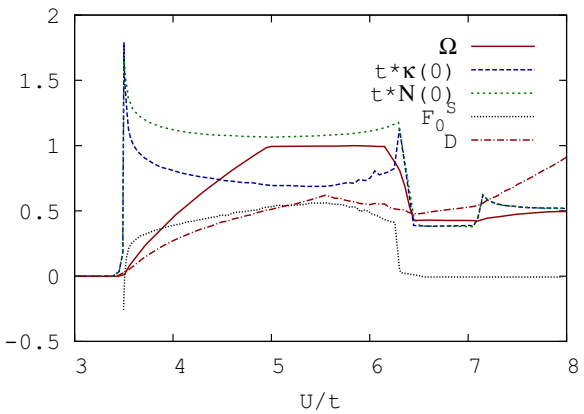

FIG. 8. (Color online) Fermi volume Ω (see text), electronic compressibility $\kappa(0)$, density of states at the Fermi level $N(0)$, the Landau compressibility parameter F_0^s, and the Drude weight D measured in units of $\frac{3te^2}{\hbar^2 a}$ in the metallic state as functions of U/t for $T/t = 0.002$.

It is worth pointing out that, according to Figs. 7 and 8, for $U/t \lesssim 4.5$ we have $\Omega \approx 4m(0)$. This result follows if we observe that, in the ground state, per unit cell there are $2m(0)$ holes in the valence band with a fixed spin projection and $2m(0)$ electrons in the conduction bands which are essentially unpolarized. Moreover, according to Fig. 7 we also have $S \approx \Omega/2$ in the same range of U. It is tempting to interpret S as the fluctuating moment of a dilute nondegenerate gas of spin-$\frac{1}{2}$ particles with density Ω.

The evolution of the electronic compressibility at low temperatures $\kappa(0)$ shown in Fig. 8 is qualitatively similar to that of the density of states $N(0)$. For $U > U_N$ we even find $\kappa(0) = N(0)$, as should have been expected, since in this region the system is fully polarized and the Hubbard model (1) is equivalent to a noninteracting system. Within Landau's Fermi-liquid theory, the electronic compressibility is related to the density of states via

$$\kappa(0) = \frac{N(0)}{1 + F_0^s},$$

where F_0^s is the Landau compressibility parameter. As already explained, for $U > U_N$ we find $F_0^s = 0$. Decreasing U slightly below U_N, F_0^s exhibits a sharp increase to a large value $F_0^s \approx 0.55$, as expected in a system with large repulsive interactions. It is quite natural that under further reduction of U, the parameter F_0^s exhibits a mild decrease. It is quite unexpected, however, that for $U \to U_c^+$ the Landau compressibility parameter becomes negative, corresponding to attractive effective charge-charge interactions in the system. A detailed study of the electronic compressibility in the vicinity of U_c will be presented elsewhere.

It is instructive to study also the optical conductivity in the limit of low temperatures. Since in the mean-field approximation we are dealing with a system of free particles, the optical conductivity contains a singular part $\sigma_{\text{sing}} = D\delta(\omega)$ where D is the Drude weight, which can be thought of as yet another measure of metallicity. If we neglect the dipole matrix elements in the calculation of $\sigma(\omega)$ as we did on the insulating side, we find $D \propto N(0)$, in agreement with the expectation that a finite density of states at the Fermi level implies a metallic state. However, since only intraband processes can contribute to the Drude weight D, it is easy to write down the full formula for D of a cubic system:

$$D = \frac{\pi e^2}{3a^3 L}\sum_{\mathbf{k}n\sigma} v_{\mathbf{k}n\sigma}^2 \delta(\varepsilon_{\mathbf{k}n\sigma} - \mu),$$

where $\mathbf{v}_{\mathbf{k}n\sigma} = \frac{1}{\hbar}\frac{\partial \varepsilon_{\mathbf{k}n\sigma}}{\partial \mathbf{k}}$ is the group velocity. The evolution of the Drude weight D with U/t is shown in Fig. 8. Note that, as expected, D exhibits a smooth increase from a vanishing value in the insulating phase to finite values in the metallic region.

Our results for Ω, $\kappa(0)$, and D, therefore, clearly show that the magnetically induced metal-insulator transition is different from the Brinkman-Rice scenario which is characterized by interaction-driven localization of charge carriers with a concomitant divergence of F_0^s. In our case it is simply the number of charge carriers which vanishes at the metal-insulator transition. However, because of its magnetic properties, the metal-insulator transition can not be identified as a simple band-crossing (or Lifshitz) transition.

IV. CONCLUSIONS

In this work we have extended the mean-field study of the minimal model [Eq. (1)] at $T = 0$, presented in Ref. [10], to finite temperatures. We have shown that, for the parameters specified by Eq. (2) which are believed to be relevant for the $FeSi_{1-x}Ge_x$ alloys, only two phases exist in the thermodynamic sense: a paramagnetic with magnetization $m = 0$ and a ferromagnetic with $m \neq 0$, separated by a quantum critical point at a critical coupling $U_c/t \approx 3.494$. The paramagnetic state at $T = 0$ is insulating, whereas the rest of the phase diagram [Fig. 2] exhibits a finite Drude weight as well as electronic compressibility, and is therefore technically metallic.

The temperature dependence of the uniform susceptibility χ in the paramagnetic phase for U close to U_c is qualitatively similar to the experimental results for FeSi [6]. The peak of χ at intermediate temperatures can be traced back to the proximity of the ordered ferromagnetic phase, thereby supporting the nearly ferromagnetic scenario for the anomalies of FeSi [9,14–16]. Furthermore, our model is also qualitatively consistent with the peculiar temperature dependence of the optical conductivity of the semiconducting compound FeSi [19,20].

Inside the ferromagnetic phase a qualitative change of the magnetization curves occurs in the vicinity of U_N, in agreement with experiments on $FeSi_{1-x}Ge_x$ [1]. Moreover, in the limit of vanishing temperature the magnetization $m(U)$ exhibits nonanalytic behavior at $U = U_N$, whose fingerprints seem to have been observed in transport properties of FeGe under pressure [24,27]. In addition, the minimal model predicts an increased density of states at the Fermi level $N(0)$ in the range $U_c < U < U_N$, again in agreement with experiments [1].

In the future it might be interesting to look for possible metamagnetic transitions in FeSi by studying the finite-B phase diagram of the minimal model. It might also be worthwhile to change the electron density ρ with the aim to describe the isostructural metallic compounds MnSi and CoSi.

It should be pointed out that the $FeSi_{1-x}Ge_x$ alloys have been described here by a model containing no disorder, which should rather describe FeGe under pressure. In order to account for the observed differences between the two physical systems, for instance, the difference between the critical volumes at the metal-insulator transition [24], it might be necessary to study a disordered version of the minimal model [Eq. (1)].

As a next step, one should test the robustness of our predictions with respect to the fluctuations which were neglected in our mean-field study of the minimal model. According to a recent variational study of the minimal model at $T = 0$ which takes some of the correlation effects into account [11], the transition from the paramagnetic insulator to the ferromagnetic metal may be weakly first order, as also suggested by the original experiments on the $FeSi_{1-x}Ge_x$ alloys [1]. Corrections are to be expected also in the paramagnetic phase close to the transition temperature T_c, since the tendency towards local moment formation is presumably not described adequately in our mean-field study. We expect that a proper treatment of such correlation effects will increase the magnetic anomalies, and, therefore, the already quite reasonable agreement between theory and experiments will further improve.

On the experimental side, the applicability of the minimal model is falsifiable in several ways. First, we suggest that the electronic specific heat of FeSi does not exhibit any peak at low temperatures. Second, we predict that the 19 GPa anomaly [24] in FeGe is caused by a cusp in the pressure dependence of the zero-temperature magnetization. Third, our results imply that the Fermi surfaces on the metallic side of the metal-insulator transition in $FeSi_{1-x}Ge_x$ should be small, and this should be visible either in angle-resolved photoemission spectroscopy or in the Hall effect measurements. Moreover, we predict that the effective charge-charge interactions in this limit should be attractive. It remains to be seen whether they can lead to superconductivity.

ACKNOWLEDGMENT

This work was supported by the Slovak Research and Development Agency under Grant No. APVV-0558-10.

[1] S. Yeo, S. Nakatsuji, A. D. Bianchi, P. Schlottmann, Z. Fisk, L. Balicas, P. A. Stampe, and R. J. Kennedy, Phys. Rev. Lett. **91**, 046401 (2003).

[2] Early studies of the alloys $FeSi_{1-x}Ge_x$ include P. Nordblad, L. Lundgren, and O. Beckman, Phys. Scr. **28**, 246 (1983); A. Bharathi, Awadhesh Mani, G. V. Narasimha Rao, C. S. Sundar, and Y. Hariharan, Physica B **240**, 1 (1997); E. Bauer, A. Galatanu, R. Hauser, Ch. Reichl, G. Wiesinger, G. Zaussinger, M. Galli, and F. Marabelli, J. Magn. Magn. Mater. **177–181**, 1401 (1998); Ch. Reichl, G. Wiesinger, G. Zaussinger, E. Bauer, M. Galli, and F. Marabelli, Physica B **259–261**, 866 (1999).

[3] L. F. Mattheiss and D. R. Hamann, Phys. Rev. B **47**, 13114 (1993).

[4] M. Krajčí and J. Hafner, Phys. Rev. B **75**, 024116 (2007).

[5] M. Neef, K. Doll, and G. Zwicknagl, Phys. Rev. B **80**, 035122 (2009).

[6] V. Jaccarino, G. K. Wertheim, J. H. Wernick, L. R. Walker, and S. Arajs, Phys. Rev. **160**, 476 (1967).

[7] R. Wäppling and L. Häggström, Phys. Lett. A **28**, 173 (1968).

[8] L. Lundgren, K. Å. Blom, and O. Beckman, Phys. Lett. A **28**, 175 (1968).

[9] V. I. Anisimov, R. Hlubina, M. A. Korotin, V. V. Mazurenko, T. M. Rice, A. O. Shorikov, and M. Sigrist, Phys. Rev. Lett. **89**, 257203 (2002).

[10] D. Plencner and R. Hlubina, Phys. Rev. B **79**, 115106 (2009).

[11] J. Imriška and R. Hlubina, Phys. Rev. B **84**, 195144 (2011).

[12] D. Vollhardt, N. Blümer, K. Held, M. Kollar, J. Schlipf, and M. Ulmke, Z. Phys. B **103**, 283 (1997).

[13] Th. Hanisch, G. S. Uhrig, and E. Müller-Hartmann, Phys. Rev. B **56**, 13960 (1997).

[14] Y. Takahashi and T. Moriya, J. Phys. Soc. Jpn. **46**, 1451 (1979).

[15] S. N. Evangelou and D. M. Edwards, J. Phys. C **16**, 2121 (1983).

[16] V. I. Anisimov, S. Yu. Ezhov, I. S. Elfimov, I. V. Solovyev, and T. M. Rice, Phys. Rev. Lett. **76**, 1735 (1996).

[17] Y. Takahashi, T. Kanomata, R. Note, and T. Nakagawa, J. Phys. Soc. Jpn. **69**, 4018 (2000).

[18] A. E. Petrova, V. N. Krasnorussky, W. M. Yuhasz, T. A. Lograsso, and S. M. Stishov, J. Phys.: Conf. Ser. **273**, 012056 (2011).
[19] D. Menzel, P. Popovich, N. N. Kovaleva, J. Schoenes, K. Doll, and A. V. Boris, Phys. Rev. B **79**, 165111 (2009).
[20] Z. Schlesinger, Z. Fisk, Hai-Tao Zhang, M. B. Maple, J. F. DiTusa, and G. Aeppli, Phys. Rev. Lett. **71**, 1748 (1993).
[21] P. Bak and M. H. Jensen, J. Phys. C **13**, L881 (1980).
[22] H. Wilhelm, M. Baenitz, M. Schmidt, C. Naylor, R. Lortz, U. K. Rößler, A. A. Leonov, and A. N. Bogdanov, J. Phys.: Condens. Matter **24**, 294204 (2012).
[23] B. Lebech, J. Bernhard, and T. Freltoft, J. Phys.: Condens. Matter **1**, 6105 (1989).
[24] P. Pedrazzini, H. Wilhelm, D. Jaccard, T. Jarlborg, M. Schmidt, M. Hanfland, L. Akselrud, H. Q. Yuan, U. Schwarz, Yu. Grin, and F. Steglich, Phys. Rev. Lett. **98**, 047204 (2007).
[25] J. J. Pulikkotil, S. Auluck, P. K. Rout, and R. C. Budhani, J. Phys.: Condens. Matter **24**, 096003 (2012).
[26] H. Yamada, K. Terao, H. Ohta, T. Arioka, and E. Kulatov, J. Phys.: Condens. Matter **11**, L309 (1999).
[27] M. Dian and R. Hlubina, Phys. Rev. B **88**, 165125 (2013).
[28] Let us note in passing that the density of states in Fig. 8 does not exhibit a smooth change in the vicinity of U_c and U_N, as should have been expected in a generic three-dimensional band structure. This is a peculiar feature of the model [Eq. (1)] with only nearest-neighbor hopping, and it should disappear in a more realistic model with longer-range hoppings.